

## OPTICAL MODELING OF A SOLAR DISH THERMAL CONCENTRATOR BASED ON SQUARE FLAT FACETS

by

**Saša R. PAVLOVIĆ \***, **Velimir P. STEFANOVIĆ**, and **Suad H. SULJKOVIĆ**

Faculty of Mechanical Engineering, University of Nis, Nis, Serbia

Original scientific paper  
DOI: 10.2298/TSCI1403989P

*Solar energy may be practically utilized directly through transformation into heat, electrical or chemical energy. We present a procedure to design a square facet concentrator for laboratory-scale research on medium-temperature thermal processes. The efficient conversion of solar radiation into heat at these temperature levels requires the use of concentrating solar collectors. Large concentrating dishes generally have a reflecting surface made up of a number of individual mirror panels (facets). Optical ray tracing is used to generate a system performance model. A square facet parabolic solar concentrator with realistic specularly surface and facet positioning accuracy will deliver up to 13.604 kW of radiative power over a 250 mm radius disk (receiver diameter) located in the focal plane on the focal length of 1500 mm with average concentrating ratio exceeding 1200. The Monte Carlo ray tracing method is used for analysis of the optical performance of the concentrator and to identify the set of geometric concentrator parameters that allow for flux characteristics suitable for medium and high-temperature applications.*

**Key words:** *parabolic dish concentrator, ray trace modeling, solar irradiation, renewable energy sources, optical efficiency, Monte Carlo method*

### Introduction

Solar radiation is an attractive source of medium-temperature thermal drive numerous industrial processes such as distributed electricity, production of heat, generation sterilization, extraction, pasteurization, drying, space cooling and heating, co-generation, tri-generation, poly-generation systems, etc. [1, 2]. The device which is used to transform solar energy to heat is referred to as solar collector. Depending on the temperatures gained by them, STC can be divided into low, medium, and high temperature systems. Analytical geometry and the Monte Carlo ray tracing method are used to analyze the optical performance of the concentrator and to identify the set of geometric concentrator parameters that allow for flux characteristics suitable for medium-temperature applications. This system is advantageous over other systems due to the absence of cosine losses. However, in practice, it is easier to fabricate a flat facet concentrator from small elementary mirrors of approximate forms, such as toroidal, spherical, rectangular, trapezoidal, square, triangle, etc. The elementary components are known as reflecting petals or facets.

---

\* Corresponding author; e-mail: saledoca@gmail.com

Saleh Ali *et al.* [3] have presented study aims to develop a 3-D static solar concentrator with a low cost and low energy substitute, to aid with the production of portable water in rural India. Optimization of the concentrator profile and geometry is also carried out to improve the overall performance; this parametric study includes the concentrator height, solar incidence angle and aspect ratio of the ellipse. The optics of a dish with mirror panels of spherical profile and uniform radius of curvature have been analyzed in paper [4]. A fundamental feature of the SG4 design [4] is the use of a single mirror panel geometry in order to reduce manufacturing and installation costs.

### Flat facet parabolic dish concentrator geometry

For the proposed solar concentrator to be used for research purposes on medium-temperature thermal processes, the radiation incident on a circular target of radius  $r_{\text{target}} = 250$  mm is required to match as closely as possible the following characteristics: radiative power of  $Q_{\text{design}} = 13.604$  kW delivered at an average concentration ratio of at least  $CR = 1200$ , and rim angle  $\psi_2$  of an axis metric cone confining radiation on the target equal to  $45^\circ$ . Consider the parabola segment shown in fig. 2 characterized by its focal length  $f$  and the rim angles  $\psi_1$  and  $\psi_2$ . Figure 1 shows an example concentrator consisting of 415 facets, placed in  $M = 12$  rows. The height  $a$  and width  $b$  of a single facet are determined for the configuration shown in fig. 3, in which the facet vertices belong to the surface of the paraboloid and the upper facet vertices of a lower row and the lower facet vertices of an upper row have the same ordinate. A parabolic dish solar concentrator (fig. 1) is a surface described by the equation: in Cartesian and cylindrical co-ordinate it is defined as:

$$Z = \frac{x^2 + y^2}{4f}, \quad Z = \frac{r^2}{4f} \quad (1)$$

$$r = \frac{2f}{1 + \cos \theta} \quad (2)$$

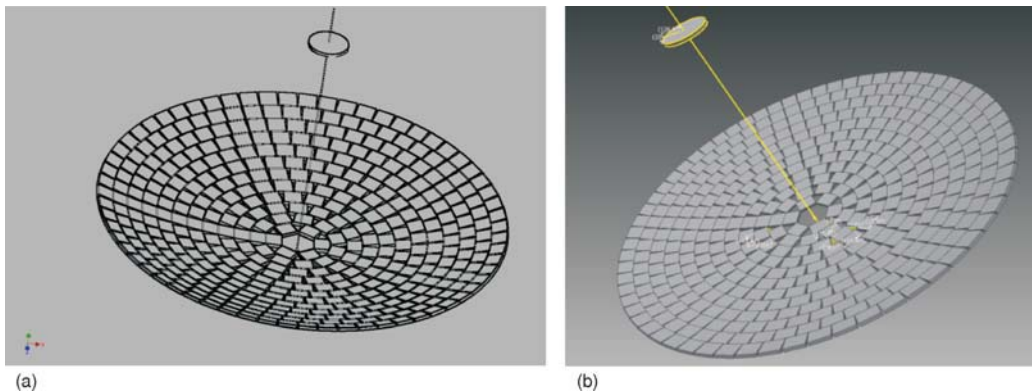


Figure 1. (a) and (b) flat square – facet concentrator: configuration with  $N_{\text{total}} = 415$  facets, placed in

The dependence between focal length and rim angle is given by the expression:

$$\frac{f}{d} = 4 \tan(\psi_{\text{rim}}^2)^{-1} \quad (3)$$

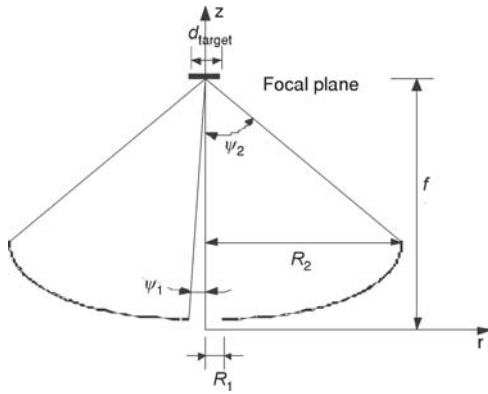


Figure 2. Schematic of truncated parabola

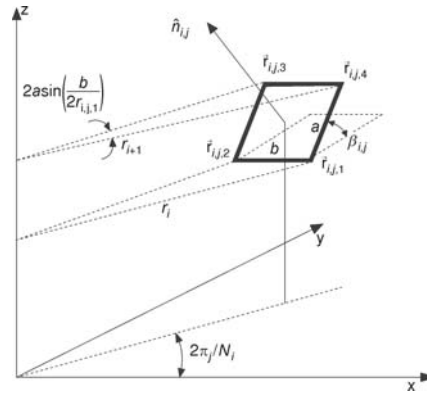


Figure 3. Plane square – facet concentrator: position and orientation of a single facet

Geometric concentration ratio can be defined as the area of the collector aperture  $A_{app}$  divided by the surface area of the receiver  $A_{rec}$  and can be calculated by eq. (4):

$$CR_g = (\sin^2 \theta_a)^{-1} = A_c A_r^{-1} = \frac{A_{app}}{A_{rec}} \quad (4)$$

The height  $a$  is found iteratively using the following optimization algorithm. The distance  $R_2 - R_1$  is divided initially into  $M$  equal intervals,  $\Delta r = (R_2 - R_1)/M = r_{i+1}^0 - r_i^0$ ,  $i = 1, 2, \dots, M$ . The facet height associated with each interval, beginning at  $k = 0$ , is calculated using the Pythagorean theorem:

$$a_i^k = \sqrt{(r_{i+1}^k - r_i^k)^2 + \frac{1}{16f^2} [(r_{i+1}^k)^2 - (r_i^k)^2]^2} \quad (5)$$

$$r_{i+1}^{k+1} = r_{i+1}^k + \delta(\bar{a}^k - a_i^k), \quad i = 1, 2, \dots, M-1, \quad \bar{a}^k = \frac{1}{M} \sum_{i=1}^M a_i^k \quad (6)$$

$0 < \varepsilon < 1$ ,  $r_{i-1}^k < r_i^{k+1} < r_{i+1}^k$ . Equations (5) and (6) are solved until the following convergence condition is satisfied:

$$\frac{1}{\bar{a}^k} \max |\bar{a}^k - a_i^k| < \varepsilon \quad (7)$$

$0 < \varepsilon < 1$ . The square facet height is set to  $a = \bar{a}^k$ , and the radius  $r_i = r_i^k$  is used for further calculations. The square facet width  $b$  is the second independent design parameter, which must satisfy the condition for the first row of facets,  $i = 1$ :

$$b \leq b_{\max} = 2R_1 \quad (8)$$

The number of facets in an arbitrary row  $i$  is then obtained from:

$$N_i = \frac{\pi}{a \sin\left(\frac{b}{2r_i}\right)} \quad (9)$$

The total number of flat facets is:

$$N_{\text{total}} = \sum_{i=1}^M N_i \quad (10)$$

In the following analysis we will limit the class of considered geometries to those based on plane square facets only ( $a = b$ ) with satisfying both eq. (9) and (10).

**Monte Carlo ray-tracing methodology**

The ray-tracing technique is used to evaluate the optical performance of a parabolic dish concentrator. During the ray-tracing analysis, all the incident rays are assumed to be parallel and carry equal energy. The vector form of reflection law of light considered in the ray-tracing technique is shown by the following equation:

$$\vec{r}_{\text{refl}} = \vec{r}_{\text{Inc}} - 2(n\vec{r}_{\text{Inc}})n \tag{11}$$

The solar ray's incident on the aperture of the concentrator can reach the receiver directly or by reflection and during the process of reflection some of the rays may be reflected back out of the concentrator. Rays may be reflected one or more times before reaching the receiver [5]. The Monte-Carlo ray-tracing methodology replicates the real photon interactions, in which stochastic paths of a large number of rays are followed as they interact with surfaces.

In the Monte Carlo ray-tracing method, the average radiation flux on the target  $\bar{q}$  and the area weighted mean solar concentration  $C_{\text{mean}}$  on a circular disk target are defined as:

$$\bar{q} = \frac{\pi \sum_{m=1}^{N_{\text{target}}} \dot{q}_m (r_m^2 - r_{m-1}^2)}{\pi R_{\text{target}}^2} \tag{12}$$

The collection efficiency  $\eta_c$ , the flux non-uniformity  $\sigma_F$ , and the average solar concentration ratio  $\bar{C}$  are defined as:

$$\eta_c = \frac{\sum_{m=1}^{N_{\text{target}}} \dot{q}_m A_m}{G_0 \pi (R_2^2 - R_1^2)}, \quad n_{\text{real, F}} = \frac{1}{j} \sum_{i=1}^j n_{\text{real, El}} \tag{13}$$

where  $N_{\text{target}}$  is the number of discrete annular elements on the circular target of total area  $A_{\text{target}}$ . The  $\dot{q}_m$  is the radiative flux intercepted by the  $m^{\text{th}}$  discrete target element,  $G_0 (I_0)$  is the incident direct solar flux – direct normal irradiance (DNI).  $\bar{q}$  is an average radiation flux on the target.  $\eta_c$  and the facet size  $a$  are simultaneously maximized while retaining acceptable values of  $\bar{C}$ . For each facet an algorithm developed in Matlab calculates a “mean” normal vector  $n_{\text{real}}$  (fig. 4) given by eq. (13). Then, values are exported to TracePro software for optical simulations. The facet co-ordinates ( $X_0, Y_0, Z_0$ ) and the ideal normal vector co-ordinates are:

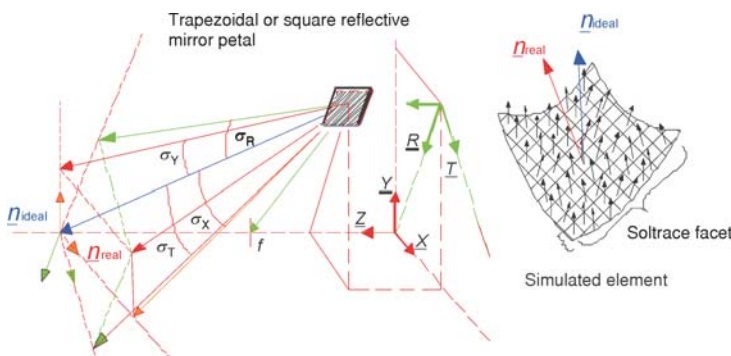


**Figure 4. Slope errors in X, Y, radial, and tangential direction**

$$F \begin{pmatrix} X_0 \\ Y_0 \\ Z_0 \equiv A_n (X_0^2 + Y_0^2) + B_n \end{pmatrix} \text{ and } \underline{n}_{\text{ideal}} \begin{pmatrix} -X_0 \\ -Y_0 \\ \frac{1}{2B_n} \end{pmatrix} \quad (14)$$

Moreover, each facet is a paraboloidal square and the focal length given by eq. 16. is equal to the distance between the parabolic dish focal length and the facet localization.

The Monte Carlo ray-tracing method is applied to compute the radiation flux  $\dot{q}_m$ . The only source of radiation is the incident solar flux in the concentrator aperture plane. Ray-tracing is a technique from geometrical optics to model the path taken by light in an environment by following rays of light. It may be used in the design of optical devices such as solar concentrators, solar optics elements, reflectors, lenses and sets of lenses in microscopes, telescopes, etc.

Table 1 represents parameters of the simulated flat facet thermal parabolic concentrator.

**Table 1. Parameters of the simulated flat plane facet concentrator**

| Parameters             | Numerical value                      | Unit |
|------------------------|--------------------------------------|------|
| Target size            | $d = 0.25$                           | m    |
| Receiver type          | Circular absorber, without shadowing | –    |
| Reflectivity of facets | 0.98                                 | –    |
| Focal distance         | 1.5                                  | m    |
| $R_1$                  | 0.125                                | m    |
| $R_2$                  | 2.5                                  | m    |
| $\theta_{\text{sun}}$  | $4.65 \cdot 10^{-3}$                 | rad  |
| $\psi_2$               | $\pi/4$                              | rad  |

$$f_F \equiv \sqrt{[X_0^2 + Y_0^2 + (f_{\text{conc.}} - Z_0)^2]} \quad (15)$$

$$\sigma_f = \frac{1}{\bar{q}} \sqrt{\sum_{m=1}^{N_{\text{target}}} (\dot{q}_m - \bar{q})^2} \frac{A_m}{A_{\text{target}}} \quad (16)$$

### Optical modeling of square-facets dish concentrator for the collector system

Random surface error  $\sigma_s$  is 0 and 10 mrad, respectively, for the facet rows  $N$  of 9, 10, 11, and 12. Thus the RMS deviation is considered for this analysis. For a given value of  $\delta_{\text{rms}}$ , the maximal square facet length  $L$  and the facet rows  $M$  are given by [5]:

$$\frac{L}{D} = \sqrt{8} \sqrt{15} \frac{\delta_{\text{rms}}}{D} \frac{F}{D} \quad (17)$$

The satisfying range  $F/D$  ratios enlarge when the facet row  $N$  increases. With the concentrator divided into a sufficiently large number of small facets, all range of  $F/D$  ratios is satis-

fyng. This relationship offers restricted limits for the  $F/D$  ratio selected for different facet rows  $N$  in the following optimization procedure of the flat square-facet parabolic concentrator.

Table 2 shows summary of reflective trapezoidal petals.

**Table 2. Summary of reflecting surface**

| Type of reflector      | Dimensions of mirrors     | Number of mirrors | Projected area of mirrors [m <sup>2</sup> ] | Concentration ratio CR ( $A_m/A_t$ ) |
|------------------------|---------------------------|-------------------|---|--------------------------------------|
| Multifaceted reflector | 100 × 100 mm flat mirrors | 415               | 9.55  | 1480                                 |
|                        | 150 × 150 mm flat mirrors | 320               | 14.45                                       | 650                                  |
|                        | 200 × 200 mm flat mirrors | 152               | 15.16                                       | 380                                  |
|                        | 250 × 250 mm flat mirrors | 74                | 13.65                                       | 225                                  |
|                        | 300 × 300 mm flat mirrors | 46                | 18.89                                       | 180                                  |

### Ray-tracing analysis of flat facet solar dish parabolic concentrator

In the optical analysis, there are two methods of calculation, analysis, and simulation of ray-trace: sequential and non-sequential ray-trace. This way of ray-trace is usually used in the so-called non-imaging optics, *i. e.* optical system that does not create an image, but are used for the concentration of optical energy. The optical software TracePro is a long-tested commercial ray-tracing code [6, 7]. In this paper an example of ray-tracing simulation on the facet solar parabolic concentrator will be shown. The flat facet parabolic solar concentrator consists of a reflector curve that is circular parabolic (obtained by rotating the parabola segment about its axis).

### Results and discussion

Figure 5(a) shows the geometric parameters of solar dish concentrator. Optical system for solar parabolic dish concentrator with traced rays is given in fig. 5(b). Figure 6 shows the

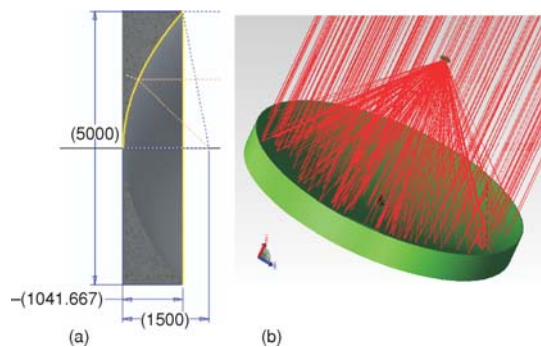


**Figure 5. (a) Geometric parameters; (b) Ray-tracing simulation of the solar dish concentrator**

variations of the collection efficiency  $\eta_c$  heat flux non-uniformity,  $\sigma_f$  and average concentration ratio  $\bar{C}$  with the target radius (diameter of receiver) for the selected number of facet rows  $M = 6, 7, 9$ , and 12, then for selected values number of specular error  $\sigma_s = 0$  mrad and 5 mrad. For  $\sigma_s = 0$  mrad a hot spot exists for each facet row number  $M$  as seen in fig. 6(a), and its radius decreases from 12 cm to 6 cm with  $M$  increasing from 6 to 12.  $\eta_c$  is approximately the same and equal to 0.74 for targets covering *hot spots* for each  $M$ .

For a realistic value of specular error  $\sigma_s = 5$  mrad, a collector efficiency of 80 %, required to satisfy the design constraints for a target of 250 mm is obtained for  $M = 7$ , corresponding to the facet size of 0.1 m and the total number of square flat facets of 415. Detail design parameters of solar parabolic dish concentrator is given in tab. 3.

**Table 3. Dimensions of a solar dish parabolic concentrator**

|   |                        |
|---|------------------------|
| Depth of the parabola   | 1.041 m                |
| Area  | m <sup>2</sup>         |
| Ideal area of the concentrator $A_{idel}$                               | ≈22,73 m <sup>2</sup>  |
| The cross section of the opening parabola $A_{pro}$                     | ≈19,63 m <sup>2</sup>  |
| A sheltered area of the concentrator $A_{shadow}$                       | ≈0,008 m <sup>2</sup>  |
| The effective area of the concentrator $A_{ef} = A_{proj} - A_{shadow}$ | ≈19,622 m <sup>2</sup> |

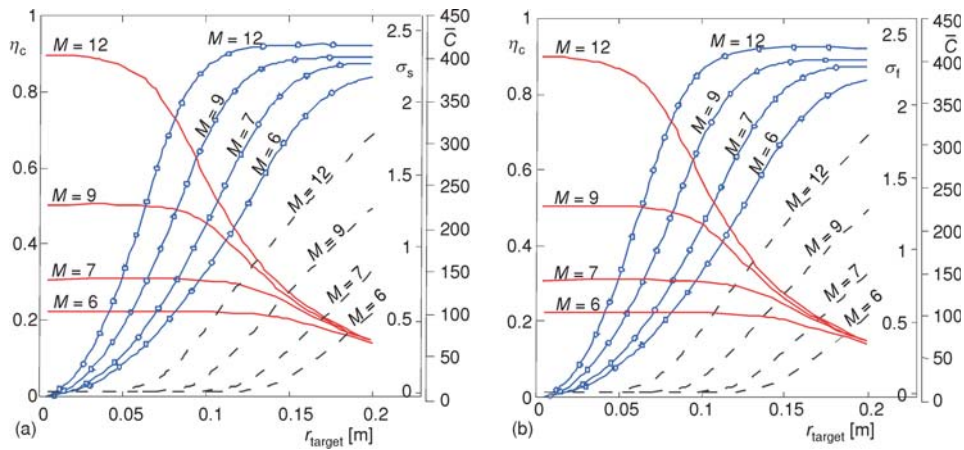


**Figure 6. Collection efficiency  $\eta_c$  (fenceline type), flux non-uniformity  $\sigma_f$  (dashed line) and average concentration ratio (continuous line) as function of target radius for  $M = 6, 7, 9,$  and  $12$  facet rows, and for specular error  $\sigma_s$ , (a)  $\sigma_s = 0$  mrad and (b)  $\sigma_f = 5$  mrad**

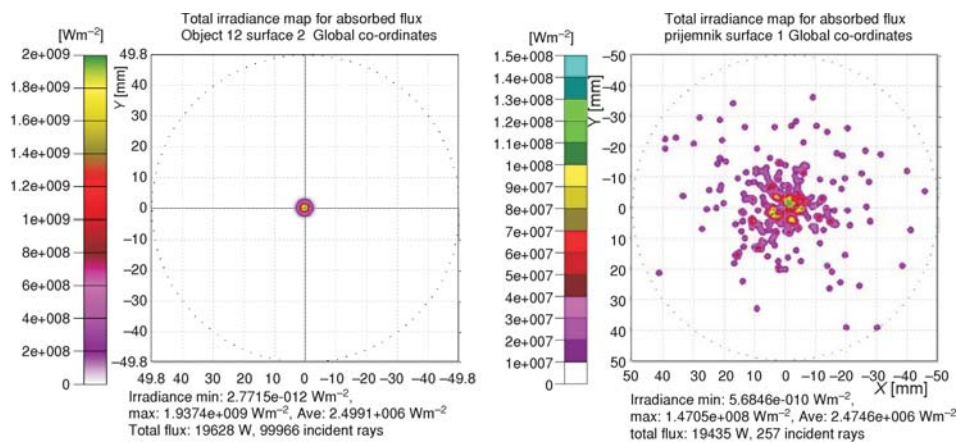


**Figure 7. Total irradiance map for absorbed solar heat flux of the flat mirror parabolic concentrator, (left – optimal total flux and total irradiance distribution  $I_b = 750 \text{ Wm}^{-2}$ ; right –  $I_b = 1100 \text{ Wm}^{-2}$ )**

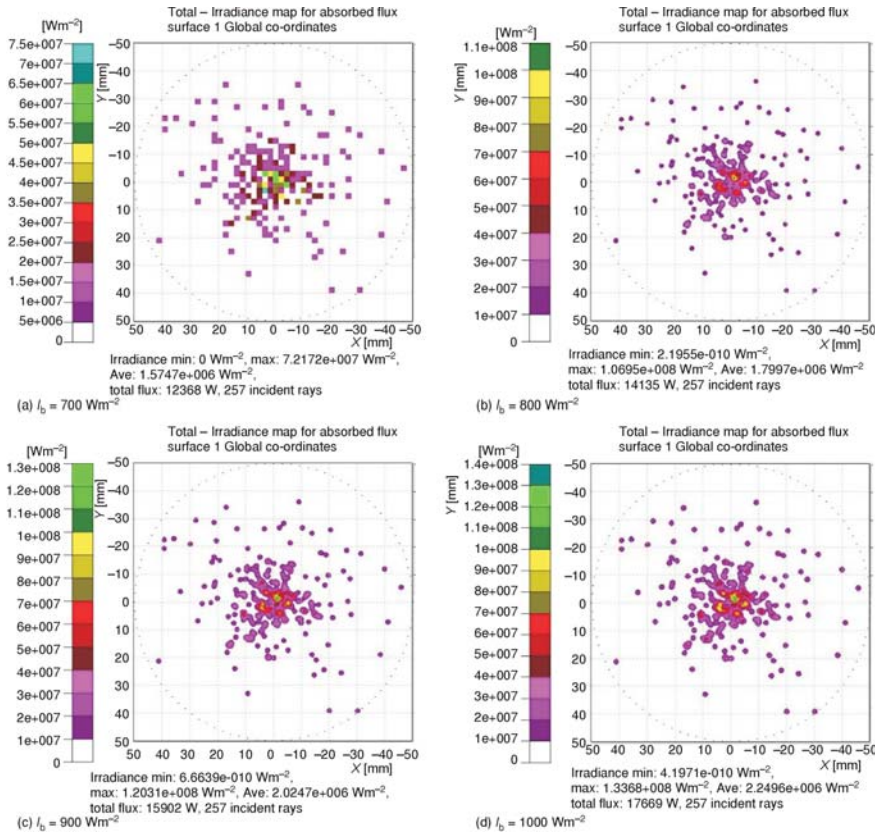


Figure 8. Total irradiance map for absorbed solar heat flux of the flat mirror parabolic concentrator

From figs. 7 and 8 one can see that calculated values for total irradiance are in compliance with theoretically values for different values of incidence radiation (direct normal irradiance). Total calculated flux on receiver was 19628 W.

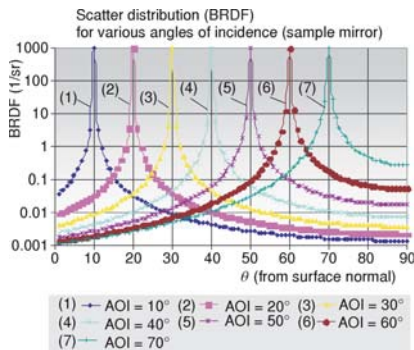


Figure 9. ABg giving the BRDF as a function of incidence angle (flat mirror)

Figure 9 shows scattered model for reflection of incidence angle for solar parabolic dish concentrator with square flat facets. In general, the reflectance of a surface increases with angle of incidence. But for a mirror, the reflectance is already very high when the AOI = 0 deg. It can not increase much more. This is why the peak BRDF does not change with AOI. However, the reflectance of a black surface increases with AOI no matter how black the surface.

Assuming a perfectly specular truncated circular and a fixed radius  $R_1 = 0.125$  m, the required total power  $Q_{design} = 13.604$  kW is obtained for  $R_2 = 2.500$  mm assuming the incident direct solar flux  $G_0 = 1000$  W/m<sup>2</sup> and the collector efficiency  $\eta_c = 80\%$ . The requirement

of  $\psi_2 = 450$  then leads to  $f = 1.500$  mm. The relationship between the size of a single facet/number of facet rows, the total number of facets and the total facet mirror area is shown in fig. 10. The total number of square facet, the total square facet area, and the number of facet rows monotonically decrease with the increasing square facet size.

### Conclusions

We have proposed a simple concept of a solar parabolic flat square facet concentrator providing irradiation for laboratory – scale research on medium – temperature conversion processes. The size and location of square facets were optimized by the Monte Carlo ray tracing analysis, in which the collector efficiency, flux non-uniformity and average concentration ratio were computed. A 415 – facet concentrator, corresponding to the facet size of 100 mm, with a realistic specular error of 5 mrad will deliver 13.604 kW over a 250 mm radius of focal region (disk target) located in the focal plane, with the average concentration ratio  $CR = 1200$ . The first direction in which the future research may go is the development and application of contemporary geometric optimizations using the Monte Carlo method and the optimization using genetic algorithms and evolution strategies using the scheme macro programming within TracePro software packages. The second direction of the future research in this area is the heat transfer analysis and simulations of thermal parameters of a receiver – absorber for a solar parabolic dish thermal collector. What will be analyzed is the impact of geometrical, optical parameters of the solar parabolic concentrators on the thermal characteristics of the absorber, and the impact of the geometrical parameters of the absorber – the receiver to heat transfer within the receiver. By using CFD modeling heat transfer and fluid flow in the absorber shall be simulated, where thermal models will be used to come to the conclusion which optical model is the best with regard to thermal efficiency of the solar thermal parabolic dish concentrator.

### Acknowledgment

This paper is done within the research framework of the research project: III42006 – Research and development of energy and environmentally highly effective polygeneration systems based on renewable energy resources. This project is financed by the Ministry of Education, Science and Technological Development of the Republic of Serbia. The authors acknowledge Lambda Research Corporation for allowing them to use the TracePro software for the Ph. D. thesis research of S. Pavlović.

### Nomenclature

|           |                               |     |                               |
|-----------|-------------------------------|-----|-------------------------------|
| $A$       | – the area, [m <sup>2</sup> ] | $b$ | – facet width, [m].           |
| $a$       | – facets height, [m]          | $C$ | – average concentration ratio |
| $\bar{a}$ | – average facet height, [m]   | $f$ | – focal length, [m]           |

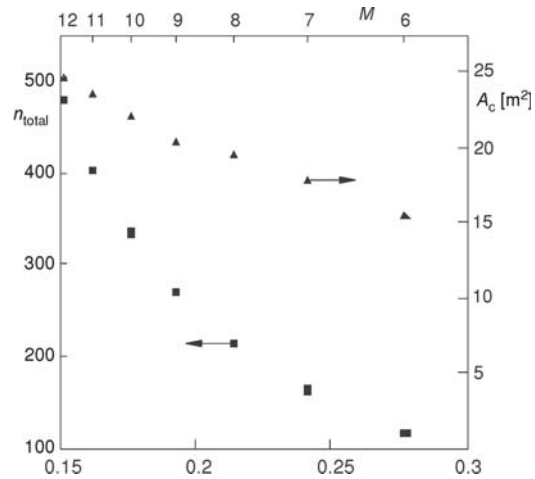


Figure 10. Total number (ntotal) of square facets (square points) and total facets area (triangular points) as functions of the facet size/number of facet rows

$G_0$  – incident direct solar flux, [ $\text{Wm}^{-2}$ ]  
 $i, j$  – indices  
 $k$  – iteration level  
 $I$  – incident radiation, [ $\text{Wm}^{-2}$ ]  
 $M$  – number of facet row  
 $N_i$  – number of facets in row  $i$   
 $N_{\text{target}}$  – number of discrete elements on target  
 $N_{\text{total}}$  – number of total facets  
 $\hat{n}$  – unit normal vector  
 $\dot{Q}$  – radiative power, [kW]  
 $\dot{q}$  – radiative flux, [ $\text{Wm}^{-2}$ ]  
 $\bar{q}$  – average radiative flux, [ $\text{Wm}^{-2}$ ]  
 $R, r$  – radius, [m]  
 $\vec{r}$  – position vector

**Greek symbols**

$\alpha$  – absorptivity, [–]  
 $\beta$  – facet tilt angle, rad; limb darkening parameter, [–]  
 $\gamma$  – constant  
 $\varepsilon$  – emissivity, small positive number, [–]  
 $\delta$  – thickness of the transparent cover, [m]  
 $\delta_{\text{rms}}$  – RMS deviation, [mrad]  
 $\delta, \varepsilon$  – small positive number  
 $\varepsilon_e$  – specify the error between two consecutive iterations, [°C]  
 $\theta$  – polar angle [rad]  
 $\theta_a$  – semi-angle reception, [°]  
 $\eta$  – the instantaneous efficiency, [%]

$\eta_c$  – collection efficiency  
 $\lambda$  – conduction coefficient, [ $\text{Wm}^{-1}\text{C}^{-1}$ ]  
 $\rho$  – reflectivity, [–]  
 $\rho^*$  – density, [ $\text{kgm}^{-3}$ ]  
 $\sigma_f$  – flux non-uniformity  
 $\sigma_R$  – slope error in radial direction  
 $\sigma_s$  – specular error  
 $\sigma_T$  – slope error in tangential direction  
 $\sigma_X$  – slope error in X-direction  
 $\sigma_Y$  – slope error in Y-direction  
 $\tau$  – transmittivity, [–]  
 $\psi_{\text{rim}}$  – rim angle [rad]  
 $\varphi, \Phi$  – azimuthal angle [rad]

**Subscripts**

b – direct radiation  
 CSE – concentrator of solar energy  
 c – environment  
 cs – circumsolar  
 d – diffuse radiation  
 ffc – flat-facet concentrator  
 sun – corresponding to sun disk  
 STC – solar thermal collector

**Acronyms**

CR – concentration ratio of solar collector  
 CSE – concentrator of solar energy  
 EHC – elliptical hyperboloid concentrator  
 DNI – direct normal irradiation

**References**

- [1] Govind, N. K., *et al.*, Design of Solar Thermal Systems Utilizing Pressurized hot Water Storage for Industrial Applications, *Solar Energy*, 82 (2008), 8, pp. 686-699
- [2] Kalogirou, S., Potential of Solar Industrial Process Heat Applications, *Applied Energy*, 76 (2003), 4, pp. 337-361
- [3] Saleh Ali, I. M., *et al.*, An Optical Analysis of a Static 3-D Concentrator, *Solar Energy*, 88 (2013), Feb., pp. 57-70
- [4] Johnston, G., *et al.*, Optical Performance of Spherical Reflecting Elements for Use with Paraboloidal Dish Concentrators. *Solar Energy*, 74 (2003), 2, pp. 133-140
- [5] Ali, I., *et al.*, Optical Performance Evaluation of a 2-D and 3-D Novel hyperboloid Solar Concentrator, in World Renewable Energy Congress, Abu Dhabi, 2010, pp. 1738-1743
- [6] Andersen, M., *et al.*, Comparison Between Ray-Tracing Simulations and Bi-Directional Transmission Measurements on prismatic Glazing, *Solar Energy*, 74 (2003), 2, pp. 157-173
- [7] Meyer, T. J. J., *et al.*, Ray Tracing Technique Applied to Modelling of Fluorescent Solar Collectors, *Proceedings of SPIE*, Vol. 7211, Physics and Simulation of Optoelectronics Devices XVII (Eds. M. Osinski, B. Witzigmann, F. Henneberger, Y. Arakawa), Bellingham, Wash., USA, 2009, pp. 1e11. doi:10.1117/12.810922.